FISEVIER

Contents lists available at ScienceDirect

Journal of Alloys and Compounds

journal homepage: http://www.elsevier.com/locate/jalcom



Crystal structure, defect chemistry and radio frequency relaxor characteristics of Ce-Doped SrTiO₃ perovskite



Burhan Ullah ^{a, b}, Wen Lei ^{a, b, **}, Xiao-Qiang Song ^{a, b}, Xiao-Hong Wang ^{a, b}, Wen-Zhong Lu ^{a, b, *}

- ^a School of Optical and Electronic Information, Huazhong University of Science and Technology, Wuhan 430074, PR China
- b Key Lab of Functional Materials for Electronic Information (B), Ministry of Education, Wuhan 430074, PR China

ARTICLE INFO

Article history:
Received 11 January 2017
Received in revised form
13 August 2017
Accepted 30 August 2017
Available online 21 September 2017

Keywords: (Sr,Ce)TiO₃ Structure ordering Dielectric property Conductivity relaxations

ABSTRACT

Crystal-defect chemistry, and temperature dependent dielectric characteristics was investigated in Cedoped SrTiO₃ (Sr_(1-3/2x)Ce_xTiO₃, x = 0.45 - 0.55) ceramics. X-ray diffraction (XRD) and transmission electron microscopy (TEM) shows the evidence of structure ordering. The samples with x = 0.45 and $x \ge 0.5$ display different phase structure evolution features with mixed- valence states of Ti³⁺/Ti⁴⁺ upon oxygen vacancy formation. The doping of Ce(x) facilitated large grain size with a dense microstructure. Activation of polar modes TO₂ and TO₄ indicated the evidence of polar nanoregions (PNRs). The system displays features of high-temperature frequency-dependent relaxor behavior rather than sharper frequency-independent normal ferroelectric anomalies. These relaxations were found to be bulk effect associated with singly (V_0^{\bullet}) and doubly (V_0^{\bullet}) charged oxygen vacancies.

© 2017 Elsevier B.V. All rights reserved.

1. Introduction

The physical nature of the ABO₃ perovskite called "incipient ferroelectric" [1,2] has attracted much attention in electronic industries for its high permittivity. One of the practically significant characteristics of polar materials is that, it has a simple crystal structure. In its unstressed, pure form, strontium titanate (SrTiO₃, ST) is an incipient ferroelectric material [1,2] in which the onset of ferroelectricity is inhibited at low temperature by quantum fluctuations and existing of the soft modes of the system never become unstable [1,2]. It remains quantum paraelectric down to ~0 K, although chemical and/or isotopic substitution, as well as the application of stress, easily disturbs this delicate state, resulting in ferroelectricity [3.4]. Experimentally, the cubic phase structure is found at high temperature, while the TiO6-octahedron rotated phase is observed below 105 K in SrTi¹⁶O₃ (ST-16) and below 110 K in SrTi¹⁸O₃ (ST-18) [5–7]. Characterization of the low temperature order parameters of these perovskite materials remain an open and engaging question. Further, judging from the fact that the ferroelectric phase (FP) is not detected in ST-16 perovskite but observed only in ST-18 below 23 k [5,8]. It was stated that SrTi¹⁶O₃ perovskite is a quantum paraelectric ceramics in which zero-point fluctuation and tunneling effect of the atomic nuclei inhibit the FP from appearing even at around 0 K. Therefore, ST material is actually quantum paraelectric in the first place; however, a FP can be stabilized under certain conditions: doping, defects, mechanical confinement, stoichiometry variations, and/or exchange of (oxygen) isotopes. Hence, the nature and temperature of the ferroelectric-paraelectric transition (FPT) in ST can be modified via partial substitution of either Sr site (A-site) and/or B-site (Ti-site) [3–11].

RE - ion A-site doped ST ceramics system has been investigated by several authors, and they found that the physical properties varied with different substitution, but the obvious improvement in the dielectric and ferroelectric response could not be obtained. On the one hand, A widely accepted viewpoint is that the relaxation and/or ferroelectric behavior in $Sr_{(1-1.5x)}Bi_xTiO_3$ (SBT) [9,10], $Sr_{(1-x)}Pr_xTiO_3$ (SPT) [3,11–13], and $Sr_{(1-x)}Ca_xTiO_3$ (SCT) [1] ceramics was due to the presence of lattice defects/impurities, including oxygen vacancies (O_{vac}), formation of polar nanoregions (PNRs) and

^{*} Corresponding author. School of Optical and Electronic Information, Huazhong University of Science and Technology, PR China.

^{**} Corresponding author. School of Optical and Electronic Information, Huazhong University of Science and Technology, PR China. E-mail addresses: wenlei@mail.hust.edu.cn (W. Lei), lwz@mail.hust.edu.cn (W.-Z. Lu).

defect centers. On the other hand, the absence of ferroelectric behavior in $Sr_{(1-3/2x)}Ce_xTiO_3$ ($x \le 0.4$) ceramics system was closely related with the existence of soft polar modes related with the incipient ferroelectric nature [2]. In summary, all these interesting and distinct results illustrate a complex coupling effects in doped $SrTiO_3$ ceramics, and have stimulated further research in this direction for its intrinsic and extrinsic mechanism.

In our previous work, the MW dielectric properties of $Sr_{(1-1.5x)}Ce_xTiO_3$ ($x \le 0.67$, sintered in air at 1350 °C) ceramics were investigated systematically. The system is characterized by $\varepsilon_\Gamma=40$, $Q\times f=5699$ GHz, and $\tau_f=+0.9$ pmm/°C [14]. The X-ray photoelectron spectroscopy (XPS) analyses of $Sr_{(1-1.5x)}Ce_xTiO_3$ ($x \le 0.67$) ceramics system revealed [14]; however, that Ce^{4+} concentration in this ceramics material is $Ce^{4+} \le 5\%$ ($Ce^{3+} \ge 95\%$) of total Ce(x) content. The existence of minor amounts of tetravalent ions (Ce^{4+}) on the Sr-sublattice under high sintering temperature should not change the chemical structure and/or defect chemistry mechanism to a significant extent.

In the present work, we report a mechanism by which relaxor phenomena can be induced via Sr-site (A-site) donor doping $Sr_{(1-1.5x)}Ce_xTiO_3$, $0.45 \le x \le 0.55$, sintered in tight closed pipe (avoid air flow). The mechanism involves substitution of Sr^{2+} ions by ceria ions, with the creation of vacancy defects in order to maintain charge neutrality. Further, the crystal structure, defect chemistry, microstructure and relaxor behavior was studied and their relationships were also discussed in detail.

2. Experimental procedure

 $Sr_{(1-3x/2)}Ce_xTiO_3,0.45 \le x \le 0.55$ were prepared by a conventional solid state method from: $SrCO_3$ ($\ge 99.9\%$ purity, Dongying J & M, Shandong, China); CeO_2 ($\ge 99.9\%$, purity, SCR, Shanghai, China); TiO_2 ($\ge 99.8\%$, purity. The starting powders were weighed according to their stoichiometric composition and were then mixed with alcohol milling for 24 h. The powders were calcined at $1200~^{\circ}C$ - $1300~^{\circ}C$ for 10 h, sieved, and re-milled overnight after adding 6 wt% binder PVA. The powders were uniaxially compacted at $100~^{\circ}C$ mm thickness in a stainless steel die, followed by cold isostatic pressing at $180~^{\circ}C$ mm the binder, followed by sintering at $1300~^{\circ}C$ - $1400~^{\circ}C$ for 3 h in a tight closed aluminum pipe (to avoid air flow).

The structure chemistry, surface morphology, defect chemistry of the sintered samples were further characterized by using X-ray powder diffraction (XRD-7000, Shimadzu, Kyoto, Japan, Cu K α ~1.5406 Å), transmission electron microscopy (TEM, Tecnai G^2 20, FEI, Oregon, and USA), scanning electron microscopy (SEM, Sirion 200; FEI, the Netherlands), Argon ion laser Raman spectrometer (Lab RAM HR800, Horiba Jobin Yvon) with a 532 nm line, and X-ray photoelectron spectroscopy (AXIS-Ultra DLD-600W, Shimadzu, Kyoto, Japan). Rietveld refinement on the XRD patterns was carried out using GSAS and powder cell software.

For dielectric measurements, the sintered samples were polished to 0.3 mm thickness; silver paste was applied to opposite faces. The Ag coated samples were fired in a furnace at 850 °C for 10 min to form the electrode. The dielectric constant and loss tangent were recorded as a function of temperature using an impedance analyzer (Agilent 4294A, Santa Clara, USA) and VDMS-2000 system (Partulab, Wuhan, China). The phase transition temperatures of the samples were investigated by differential scanning calorimetry (DSC, NETZSCH STA 449F3 Germany). The hysteresis loop (*P-E* loop) response was measured at room temperature using the Radiant Mulitiferroic devices (RT66 B, Radiant Technologies, USA).

3. Results and discussion

The XRD spectra of $Sr_{(1-3x/2)}Ce_xTiO_3$ ceramics with x = 0.45 may be indexed according to a tetragonal unit cell with tetragonality ratio (c/a) of ~0.999 (Fig. 1 and Table 1). The splitting of the (310) peak reflection (x = 0.45) clearly demonstrates that, the resulting symmetry is therefore lower than cubic (C-phase), and is probably tetragonal (T-phase, x = 0.45) [14.15]. Besides this, Rietveld refinements are carried out for x = 0.45 to further analyze the crystal structure (Fig. 2). The X-ray diffraction spectra were refined based on the tetragonal in space group P4/mmm with refined reliability factors ($R_{\rm wp}=7.5\%$, $R_{\rm p}=5.9\%$, and $\chi^2=2.1\%$) together with the structure lattice parameters suggested that $Sr_{(1-3x/2)}Ce_xTiO_3$ (x = 0.45) crystallized into the tetragonal structure (Table 1). The structure of $Sr_{(1-3x/2)}Ce_xTiO_3$ (x = 0.45) indicates that Ce atom are twelve-coordinated while the Ti atom coordinates with six-oxygen forming (TiO₆)-octahedral environment (Fig. 2). On the other hand, for $x \ge 0.5$, splitting of the (200) peak along with the appearance of structure ordering indicated an orthorhombic structure (Ce_{0.6}TiO₃, Pmmm (47), JCPDS # 70-3939) (Fig. 3). The clue to the orthorhombic phase structure at $x \ge 0.5$ arises from the existence of an extra superlattice reflections and the splitting of high angle peak, both of which cannot be accounted for cubic and/or tetragonal phase structure [14–16]. The splitting of the Bragg reflection at higher 2θ angle and the presence of Ovac then gives rise to the question of a possible structure ordered arrangement of these vacancies. In fact, the appearance of the superlattice peaks consistent with antiphase tilting reflection (α), antiparallel displacement of the A-site cation (β) , and in-phase tilt reflections (i) could be resulted from cell doubling due to octahedral tilting and/or oxygen vacancy ordering [14,16]. Alternatively, the compositional ordering (superstructure lattices) of the type 1/2{000}, 1/2{ee0} and 1/2{00e} accompanies distortion of the TiO₆, resulting in the change of symmetry from tetragonal down to orthorhombic [14-16].

A shift to higher angles was observed in the main (110) peak, which shows the shrinkage of the lattice due to the substitution by cerium of A-site cation (Sr-site). However, at x=0.5 the (110) peak slightly shift towards lower angle, which could be due the incorporation of the smaller Ce^{4+} ($r_{11}^{4+}=0.87$ Å, CN=6) in place of Ti^{4+} ($r_{11}^{4+}=0.605$ Å, CN=6) at B-site. However, taking into account, the computer simulation studied on Strontium-Titanate (SrTiO₃) [17], rather than the ionic radii of Sr^{2+} ($r_{Sr}^{4+}=1.44$ Å) and Ce^{4+} ($r_{Ce}^{4+}=0.87$ Å), it was revealed that the presence of minor amount of

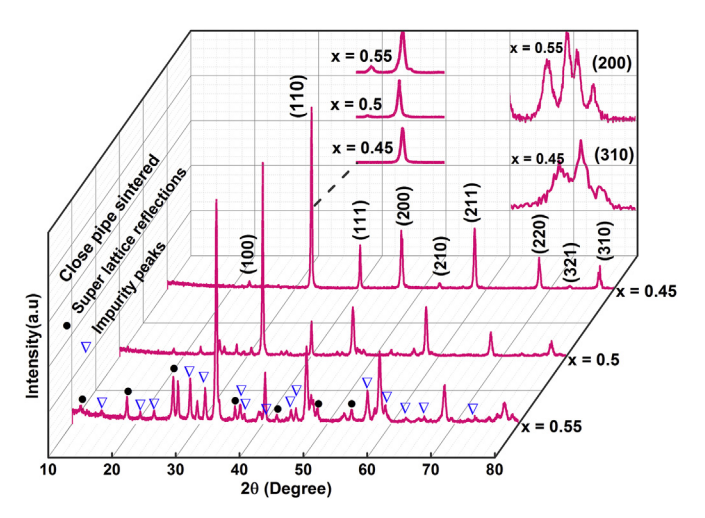


Fig. 1. X-ray diffraction patterns for $Sr_{1-3/2x}Ce_xTiO_3$ (0.45 $\leq x \leq$ 0.55) ceramics. The insert figure shows, the peaks splitting and peak shifting in (310), (211), and (110) reflections.

Download English Version:

https://daneshyari.com/en/article/5458180

Download Persian Version:

https://daneshyari.com/article/5458180

Daneshyari.com